

Inter-layer slide and stress relaxation in a bilayer fluid membrane in the patch-clamp setting.

Sergei I. Mukhin and Svetlana V. Baoukina

Theoretical Physics Department, Moscow Institute for Steel and Alloys,
Leninskii pr. 4, 119991 Moscow, Russia

Running title: Inter-layer slide and stress relaxation

Keywords: bilayer lipid membrane, mechanosensation, lateral stress relaxation, interlayer slide, MscL gating, thermal activation

Abstract

Protein mechanosensitive channels (MS) are activated by tension transmitted through the lipid bilayer. We propose a theory of lateral stress relaxation in a bilayer lipid membrane exposed to external pressure pulse in the patch-clamp experimental setting. It is shown that transfer of lipid molecules into a strained region is thermodynamically advantageous due to local decrease of the stress. Considered stress relaxation mechanism may explain recent experimental observations (Davidson and Martinac 2003) of adaptation of MscL, bacterial mechanosensitive channel of large conductance, to sustained membrane stretch. Lateral stress relaxation in the monolayer, which controls the gating of MscL, triggers thermally activated transition of the open channels back to the closed state ("adaptation"). We evaluate the contribution of the hydrophobic mismatch between MS channel and lipid bilayer to the energy barrier separating open and closed states. Then, using the MscL thermodynamic model (Sukharev et. al, 1999), we estimate characteristic adaptation times at room temperature to be of the order of seconds, well in the range of the experimental data (Davidson and Martinac 2003). Estimated propagation time of the initial channel-opening stress over the whole membrane is 4-5 orders of magnitude shorter.

I. INTRODUCTION

The functioning of the protein channels in the cell membranes regulates flows of ions in- and out of the cell, thus influencing signal transmission in the neural networks (Doyle et al., 1998; Ming Zhou et al. 2001). Mechanical stresses in the cell membranes control gating of the protein mechanosensitive (MS) channels (Sukharev, 2001), which hence play a role of mechanoreceptors in the cellular organisms. Therefore, a theory of the stress propagation and relaxation in the lipid bilayer membranes is of substantial interest for the fundamental and practical purposes (Yeung and Evans, 1995; Cantor, 1999). One of the biological objects convenient for experimental study is the large conductance MS channel (MscL) in the inner membrane of the *Escherichia coli* (E-coli) bacteria. It is possible to measure a single channel conductance, and find its dependence on the internal lateral tension in the membrane. The tension, which causes opening of the channel, could be evaluated using video microscopy measurements of the membrane curvature formed under the applied external pressure (Sukharev et al., 1999).

The time-dependence of the membrane's conductance observed in (Hase et al., 1995) and (Davidson and Martinac, 2003) reveals gradual collapse of the ionic currents through the MscL's (called adaptation) within seconds after their opening. According to existing hypothesis (Sachs and Morris, 1998), this may happen due to mutual slide of the lipid monolayers, constituting a bilayer membrane of

the E-coli. This slide would then cause a relaxation of the channel-opening lateral stress inside the membrane. Thus, the slide of the monolayers is induced by the same pressure pulse, which leads initially to the opening of the MscL's.

In this paper we propose a theory of such a stress-relaxation process and demonstrate that the slide of the monolayers after application of a constant external pressure gradient across the membrane is indeed thermodynamically advantageous. In Section II we outline the main physical ideas and mechanisms considered in this paper. In particular, we apply the theory of the interlayer slide dynamics (Yeung and Evans, 1995) in order to evaluate characteristic time of the stress-relaxation process. We also show that characteristic time of the MscL adaptation following the stress-relaxation in the membrane is actually much longer. In general, this is caused by the necessity of a thermal activation involved in the channel adaptation process. Using the MscL thermodynamic model (Sukharev et. al, 1999), we estimate characteristic adaptation times at room temperature to be of the order of a few seconds, well in the range of the recently reported experimental data (Davidson and Martinac 2003).

In Section III we introduce a model free energy functional of a bilayer membrane. We add to the free energy an adhesion energy term, which reflects important feature of the patch-clamp experimental setting regarding adhesion of the lipid monolayer to the glass wall of the pipette. Then, the self-consistent calculation procedure is outlined of the membrane free energy in the semi- and complete equilibrium states under a constant pressure gradient in a patch-clamp setting. In Section IV we consider results of our numerical calculation of the free energy difference between the two successive semi- and complete equilibrium conformations of a membrane, i.e. : (1) after application of a constant external pressure gradient, but before the interlayer slide; and (2) after the slide of one monolayer with respect to the other, leading to the complete equilibrium conformation. The influence of the adhesion of the lipids to the glass wall of the pipette is also studied numerically. Results reasonably compare with the experimental data.

In Section V we review our main estimates of the time scales characterizing the membrane and the MscL dynamics. Also, the effect of the energy barrier separating open and closed states of the MscL on its adaptation to sustained stress is discussed. The difference between MscL adaptation in the thick and thin lipid bilayers is considered in relation with the experimental data for the PC-20 and PC-18 liposome patches described in the companion paper (Davidson and Martinac 2003).

Possible experimental verifications and future improvements of the theory are also discussed. We focus on the physical ideas in the main text and place more detailed mathematical derivations in the appendices.

II. BILAYER LIPID MEMBRANE WITH MSCL: CHARACTERISTIC TIME SCALES

A. The shortest time

The first, semi-equilibrium conformation of a bilayer in the patch-clamp setting is achieved shortly after application of a pressure difference pulse P , within the time of propagation of the mechanical stress along a membrane: $\Delta t \sim \omega_b^{-1} \sim 10^{-5} \div 10^{-4} \text{sec}$. Here characteristic bending frequency ω_b is evaluated below in Eqs. (65) and (64) using the theory of bending waves in a thin plate. In the semi-equilibrium state under consideration the number of the phospholipid molecules in the curved part of the bilayer membrane has increased relative to the initial flat conformation mainly due to a tearing off the membrane from the walls of the pipette, see Fig. 1. In order to allow for this, a finite adhesion energy, E_{ad} , is introduced below. The tensions T_1 and T_2 in the two monolayers of the membrane approximately coincide, since the radius R of the membrane is of the order of $1 \div 5 \mu\text{m}$, while its thickness, $2 \cdot l_0$, is about (Hase et al., 1995) $3.5 \div 4 \text{nm}$. Hence, on such a short time scale Δt the membrane behaves effectively like a unit structure, as if the monolayers are strongly coupled together and can not slide with respect to one another.

B. The lateral stress relaxation time

Described conformation is a semi-equilibrium one because it possesses a tension gradient along the surface of the lower monolayer 1. The gradient $\nabla_s T_1$ arises as long as the tension in the curved part of the membrane (in the pipette) is finite: $T_1 \neq 0$, while it is zero in the rest of the patch, see Fig. 1. Hence, layer 1 will slide against layer 2 (the latter is stuck to the walls). A sliding velocity v_s is determined by the drag coefficient (Yeung and Evans, 1995) b :

$$bv_s = \nabla_s T_1 = K_A \nabla_s \alpha, \quad (1)$$

where K_A and α are area compressibility modulus for monolayer and dilation field respectively ($\alpha \equiv a/a_0 - 1$ where a is the area per lipid molecule). Then, a conservation equation for the dilation field takes the form of a diffusion equation:

$$\frac{\partial \alpha}{\partial t} = \nabla_s v_s \equiv K_A \nabla_s^2 \alpha \equiv D \nabla_s^2 \alpha ; D = \frac{K_A}{b}, \quad (2)$$

where D plays the role of a diffusivity constant of the dilation field. Then, the lateral stress relaxation time, τ_s , which is necessary for the dilation field to level off diffusively between the outer patch and the center of the curved membrane along the distance $\sim R$ is evaluated as:

$$\tau_s \sim \frac{R^2}{D} \sim \frac{R^2 b}{K} \sim \frac{2R^2 b \bar{\alpha}}{T_1} \sim \frac{1.2 \cdot 10^{-7} \text{cm}^2 \cdot 10^7 \text{dyn} \cdot \text{sec}/\text{cm}^3 \cdot 0.05}{6 \text{dyn}/\text{cm}} = 0.01 \text{sec}, \quad (3)$$

where we evaluate $K_A \sim T_1/\bar{\alpha}$. The characteristic area dilation per lipid, which does not destroy the membrane, is evaluated as $\bar{\alpha} \leq 0.05$. A typical value of b for a flat membrane is (Yeung and Evans, 1995) $\sim 10^7 \text{ dyn} \cdot \text{sec}/\text{cm}^3$. Measured value of external pressure (Sukharev et al., 1999) is about 50 mmHg , which corresponds to the membrane's lateral tension $T = 11.8 \text{ dyn}/\text{cm}$ at the curvature radius $r \sim R \approx 3.5 \mu\text{m}$. Hence, the instantaneous tension in the monolayer 1 is: $T_1 = T/2 \sim 6 \text{ dyn}/\text{cm}$, thus leading to above estimate of the lateral stress relaxation time τ_s .

The time τ_s may become even greater if interdigitation between the monolayers increases in the curved-stretched conformation of the membrane. The effective drag coefficient b may also be enhanced due to an extra impedance caused by a finite density of the protein channels piercing the membrane.

The estimate in Eq. 3 is still considerably shorter than the experimental adaptation times $\sim 1 \text{ sec}$ (Hase et al., 1995), (Davidson and Martinac 2003). In order to understand the reason for such a difference one has to allow for additional factor influencing the MscL adaptation time. After the relaxation of the lateral tension T_1 in the lower monolayer the MscL has to overcome a (free)energy barrier to make transition from the open to the closed state. This transition, as is estimated below, requires time, which, indeed, proves to be much longer than τ_s .

C. The MscL adaptation time

The structure of MscL is assymmetric and the cytoplasmic half of the channel poses a barrier to ion permeation (Sukharev et al., 2001). This half of the channel is situated in the lower monolayer of the membrane in the considered experimental settings (Sukharev et al., 1999; Hase et al., 1995). Hence, activation/closing of the MscL is regulated by the lateral tension T_1 in this lower monolayer 1. Let us use a simple elastic model of MscL channel (Sukharev, Sigurdson et al., 1999) to study the kinetics of the channel closing induced by interlayer slide. A detailed derivation is presented in the Appendix B (see also Fig. 4). Here we merely describe the main consequences. The value of the rate constant for the open to closed transition, k_c , is the key factor:

$$k_c = \tilde{k} \exp \{ -E_{act,c}/k_B T_0 \} , \quad (4)$$

where k_B is Boltzmann's constant, T_0 is temperature, \tilde{k} is "attempt rate". The activation barrier for closing of the channel starting from the open state equals (see Appendix B, Eq. (B8)):

$$E_{act,c}(T) = \frac{B_0}{2}(A_0 - A_b)^2 + T(A_0 - A_b) + \frac{T^2}{2B_0} \quad (5)$$

where T is lateral tension stretching the channel; $A_0 > A_b$ designate the areas of the pore in the open and top-of-the-barrier conformations respectively; B_0 is elastic constant of the channel in the open state. The parabola Eq. (5) has minimum at $T < 0$. Hence, the activation barrier for the channel closing remains

finite (does not reach zero) within the interval of non-negative tensions ($T > 0$). Simultaneously, we find that relaxation of the tension T_1 in the lower monolayer favours closing of the MscL with the rate k_c defined in Eq. (4), as $E_{act,c}$ in (5) decreases with the decrease of T . The pre-exponential factor \tilde{k} in Eq. (5) may be estimated as $\sim 100sec^{-1}$ (Sukharev and Markin, 2001). Then, regarding adaptation time as the equilibration time of the initially open channel $\tau_{eqv} = k_c^{-1} \sim 1.5sec$ (Davidson and Martinac, 2003)), triggered by the relaxation of lateral stress in the lower monolayer, we estimate the order of magnitude of the activation energy $E_{act,c}$ inverting Eq. (4):

$$E_{act,c} = k_B T_0 \ln \tilde{k}/k_c \equiv k_B T_0 \ln \{\tilde{k}\tau_{eqv}\} \approx k_B T_0 \ln\{150\} \approx 5k_B T_0. \quad (6)$$

We show in Section V that this value of $E_{act,c}$ has the relevant scale for the known set of the thermodynamic parameters characterizing the MscL channels.

D. The MscL activation time

The necessity to overcome a free energy barrier may also increase MscL transition time from the closed to the open state (MscL activation time). Remarkably, unlike in the case of adaptation, the height of the barrier for MscL activation may vanish at finite tension $T^* > 0$. Thus, the lateral tension T enhances MscL opening rate, and the latter process may happen without the thermal activation. Using the same elastic model as in Eqs. (4)-(5) above, we find expression for the rate constant of the closed to open state transition, k_o :

$$k_o = \tilde{k} \exp \{-E_{act,o}/k_B T_0\}, \quad (7)$$

where \tilde{k} is "attempt rate" in the closed state. The activation barrier for opening of the channel starting from the closed state equals (see Appendix B, Eq. (B9)):

$$E_{act,o}(T) = \frac{B_0}{2}(A_b - A_C)^2 - T(A_b - A_C) + \frac{T^2}{2B_C}, \quad (8)$$

where A_b designates the area of the pore in the closed MscL conformation; B_C is elastic constant of the channel in the closed state. The maximal value $E_{act,o}(T)$ possesses at $T = 0$:

$$E_{act,o}(T = 0) = \frac{B_0}{2}(A_b - A_C)^2, \quad (9)$$

see Fig. 4. The minimal value $E_{act,o}(T) = 0$ is reached at $T = T^*$, where :

$$T^* = B_C(A_b - A_C); \quad E_{act,o}(T \geq T^*) = 0. \quad (10)$$

Hence, it follows from Eqs. (7) and (9), (10) that activation time $\tau_a \sim k_o^{-1}$ changes from its maximal value $\tau_a(T = 0)$ at zero tension down to its shortest value at $T \geq T^*$:

$$\tau_a(T) = \begin{cases} \tilde{k}^{-1} \exp \{B_0(A_b - A_C)^2/2k_B T_0\}, & T = 0 \\ \tilde{k}^{-1}, & T \geq T^* \end{cases}$$

Indeed, according to (Sukharev, Sigurdson et al., 1999), an increase of T from $11.9mN/m$ to $14.14mN/m$ leads to a decrease of the activation time $\tau_a \sim k_o^{-1}$ by about 40 times, so that it reaches the absolute value of $6.8 \cdot 10^{-3}sec$.

E. The lipid diffusion time

We have also calculated the free energy of the whole patch: bent part and unstrained outer part, as a function of the external pressure difference P in both the semi- and complete equilibrium states. Indeed, the free energy in the relaxed, $T_1 = 0$ state, proves to be lower than in the semi-equilibrium state achieved before the slide, Fig. 2a. A comparison of the calculated numbers N_1 and N_2 of the lipids, in the curved lower and upper monolayers correspondingly, in the semi- and complete equilibrium states follows from Fig. 2b. It shows that the number ΔN_1 of the lipids "sucked in" from the patch to relax T_1 is of a macroscopic magnitude, e.g. $\Delta N_1 \sim 4\%N_1$. Based on these result, we estimate also a diffusion time, τ_d , which would be necessary for the lipid molecules to move from the patch to the monolayer 1 chaotically, i.e. without the slide motion of the monolayer as a whole. Experimentally determined diffusion coefficient of the individual lipid molecules in bio-membranes at room temperature is (Sonnleitner et al., 1999): $D \sim 1 \div 10\mu m^2/sec$. Hence, we evaluate a characteristic diffusion time τ_d as:

$$\tau_d \sim (\Delta N_1/N_1)R^2/D \sim 0.1 \div 1sec, \quad (11)$$

which is by orders of magnitude longer than the sliding time τ_s , Eq. 3. Hence, diffusion of individual lipid molecules proves to be less effective for the relaxation of the stress in the concave monolayer than the interlayer slide.

F. Adaptation in PC-20 *versus* no adaptation in PC-18

Despite the seeming clarity of the mechanisms, which determine the different time scales described above, the whole picture of MscL response to the sustained lateral tension in the membrane can be more involved: hydrophobic mismatch affects MscL gating (Perozo et al., 2002). While MscL exhibited adaptation in bilayer formed with diacosenoyl phosphatidylcholine, PC-20 molecules, no adaptation to sustained stress was observed in bilayer made of dioleoyl phosphatidylcholine, PC-18 (Davidson and Martinac 2003). Below we present some estimates demonstrating that the change of MscL hydrophobic mismatch between its closed and open conformations can be responsible for a fairly different gating behavior depending on whether the lipid bilayer is "thick" or "thin". This may explain experimentally observed drastic difference between MscL gating behaviors in PC-20 and PC-18 bilayers. We use here again the elastic model of MscL channel (Sukharev and Mrkin, 2001) in combination with the lipid-protein hydrophobic

mismatch model (Fournier, 1999) shortly introduced in the Appendix.

The length of hydrophobic region of (the external wall) MscL channel is different for its closed and open conformations (Sukharev et al., 2001). The mismatch energies in the open and closed states of the MscL channel, F_{LP}^O and, F_{LP}^C , contribute to the total free energy of these conformations, F_O and F_C . The free energy difference between open and closed states is then given by:

$$F_O - F_C = \tilde{E}_0 + \Delta F_{LP}, \quad (12)$$

here $\Delta F_{LP} = F_{LP}^O - F_{LP}^C$ is the part of the energy difference arising from the difference in hydrophobic mismatch energies, while \tilde{E}_0 is determined by other factors (Sukharev, Sigurdson et al., 1999), e.g. the type of lipids in the bilayer (hydrocarbon chains length; curvature stress profile), thermodynamic conditions of the surrounding solution (pH, temperature). In the elastic model of MscL at $T = 0$: $\tilde{E}_0 + \Delta F_{LP} = E_0$. The mismatch energy depends on the type of lipid; if the length of the lipid tail provides better matching of lipid-protein hydrophobic regions, this results in lower mismatch energy and lower total energy of the given channel conformation. In other words, lipids surrounding the channel favour certain (closed or open) conformation of the MscL (Hamill and Martinac, 2001).

For example, if in the (initial) closed state of MscL the hydrophobic thickness of the bilayer is equal or greater than that of the channel, the channel opening increases the mismatch and, thus, the mismatch energy adds to the value E_0 (and to the energy separation $F_O - F_C$). On the other hand, if the hydrophobic thickness of the bilayer is less or matches that of MscL in the open conformation, the channel opening decreases the mismatch and, hence, the mismatch energy subtracts from E_0 . In the thermodynamic model of MscL it corresponds, see Fig. 4, to the decreased vertical distance (i.e. E_0 at $T = 0$) between the parabolas describing the free energies of the open and closed conformations of the channel. When MscL opens, its hydrophobic thickness decreases by $6 \div 8 \text{ \AA}$ (S. Sukharev, Maryland University, personal communication, 2003). Our estimate (see Appendix B) shows, that the difference of mismatch energies between open and closed states of MscL, ΔF_{LP} , may range up to $20k_B T$.

We would expect that shorter lipids (e.g. PC-18 compared to PC-20) favour open state of MscL:

$$(\Delta F_{LP})^{PC18} < (\Delta F_{LP})^{PC20}. \quad (13)$$

This implies that the energy difference, $F_O - F_C$, becomes smaller:

$$(F_O - F_C)^{PC18} < (F_O - F_C)^{PC20}. \quad (14)$$

Thus at any tension the ratio of the equilibrium fractions of the open and closed channels, n_O/n_C :

$$n_O/n_C \sim \exp \{-(F_O - F_C)/k_B T_0\} \quad (15)$$

is shifted towards increased fraction of open channels n_O for PC-18 as compared to PC-20 :

$$(n_O/n_C)^{PC18} > (n_O/n_C)^{PC20}. \quad (16)$$

This is why in PC-18 liposome an interlayer slide (and resulting relaxation of the lateral tension in the lower monolayer) may not lead to a complete closing back of the MscL's in the final thermodynamic equilibrium state, since at $F_O \approx F_C$ we have $n_O/n_C \sim 1$. We also expect the closing of (a fraction of) MscL's to take longer time in PC-18 bilayer in comparison with PC-20 bilayer as the energy barrier between closed and open conformations, $E_{act,c}$, increases with a decrease of E_0 , Fig. 5 (see explanation in Appendix B after Eq. (B9)). The higher energy barrier leads to the lower rate of closed-to-open transition, k_c in Eq.(4).

G. Interlayer slide and hydrophobic mismatch

Interlayer slide makes no significant contribution to the energy of hydrophobic mismatch. Due to the incompressibility condition, $V = a \cdot l = const$ (V - is volume of lipid molecule, a - is area per lipid molecule, l -is lipid length in the strained membrane), tension in each monolayer, T_i , produces fractional change in its thickness:

$$T_i = -\frac{\Delta l}{l_0} \cdot K_A. \quad (17)$$

Here $i = 1, 2$ is monolayer label; $\Delta l = l - l_0$, and l_0 is the length of a lipid in the unstressed flat membrane; K_A is the area compressibility (expansion) modulus of a monolayer. After the application of external pressure, P , to the membrane (but before interlayer slide) both monolayers are strained and tensions in them approximately coincide:

$$T_1 \approx T_2 \approx T/2, \quad (18)$$

here T is tension in the membrane defined according to Laplace law: $T = Pr/2$, r is curvature radius. The total relative change in membrane thickness, is given by:

$$\frac{\Delta l_1 + \Delta l_2}{2l_0} \approx \left[-\frac{T_1}{2K_A} \right] + \left[-\frac{T_2}{2K_A} \right] = -\frac{T}{2K_A}. \quad (19)$$

After the interlayer slide the flow of lipids from the unstrained outer patch to the lower monolayer leads to the relaxation of lateral stress in it; tensions are redistributed:

$$T_1 = 0, \quad T_2 = T. \quad (20)$$

But the total change in the bilayer thickness, evidently, remains nearly the same:

$$\Delta l_1 = 0, \quad \frac{\Delta l_2}{2l_0} \approx -\frac{T}{2K_A}. \quad (21)$$

III. THE MODEL FREE ENERGY OF MEMBRANE

We start from the microscopic model of a bilayer membrane as described e.g. in (Safran, 1994; Ben-Shaul, 1995; Xiang and Anderson, 1994). First, write a single i -th monolayer ($i = 1, 2$) free energy per lipid molecule f_i :

$$f_i = f_{si} + f_{hi} + f_{ti} \equiv \gamma a_i + C/a_i + (k_s/2)(l_i - l_s)^2 \quad (22)$$

Here f_{si} is the external surface energy of the monolayer, which increases with the area per lipid molecule a_i due to the hydrocarbon tails interaction energy with the solvent. The short-range repulsion between the polar molecular heads at the surface of the membrane is represented by the second term in Eq. 22. The third term, though looks like a spring elastic energy (with not stretched spring length l_s), codes for the entropic repulsion between the hydrocarbon tails in the depth of each monolayer (Safran, 1994). In what follows we omit the second term in Eq. 22 on the empirical grounds (Ben-Shaul, 1995) relevant for the chain molecules in phospholipid bilayers. There is no interface energy term included in Eq. 22 for the internal surfaces of the monolayers forming the bilayer, as the latter are not reachable for the solvent molecules. We also assume a vanishing interdigitation of the tails between the adjoint monolayers. The length of a lipid molecule l_i , i.e. the thickness of the i -th monolayer, is not an independent variable from the area per molecule a_i . The volume v per lipid molecule is conserved, i.e. the latter could be considered as incompressible (Safran, 1994; Ben-Shaul, 1995). Due to this conservation condition the length l_i is related to the mean and gaussian curvatures H and K at the interface between the monolayers by a well known differential geometry formulas (Safran, 1994) :

$$l_1 = l_{01} - l_{01}^2 H + (2/3)l_{01}^3 K \quad (23)$$

$$l_2 = l_{02} + l_{02}^2 H + (2/3)l_{02}^3 K \quad (24)$$

Here the change of sign in front of H -term in the equation Eq. 24 relative to that in equation Eq. 23 is due to a simple geometrical fact that the *external* normal vector to e.g. the layer 1 is simultaneously an *internal* normal vector to the layer 2 at their mutual interface. Different l_{0i} parameters just reflect the incompressibility of the lipid molecules mentioned above:

$$l_{0i} = v/a_i \quad (25)$$

Substituting Eqs. 23 and 24 into the third term of Eq. 22 one finds contributions to the free energy from the tails in the form:

$$f_{t1} = (k_s l_{01}^4 / 2) \left[(H - C_{01})^2 + (4/3)C_{01} l_{01} K \right] \quad (26)$$

$$f_{t2} = (k_s l_{02}^4 / 2) \left[(H + C_{02})^2 + (4/3)C_{02} l_{02} K \right] \quad (27)$$

where parameters C_{0i} have the meaning of the local spontaneous curvatures of the i -th layer:

$$C_{0i} = (l_{0i} - l_s)/l_{0i}^2 \quad (28)$$

We readily recognize the Helfrich's formula (Zhong-Can and Helfrich, 1987; Zhong-Can and Helfrich, 1989) for the free energy of a membrane in Eqs. 26 and 27.

In a symmetric bilayer case the numbers of lipids in the 1-st and 2-nd monolayer are equal: $N_1 = N_2$. Under the equivalent conditions on the opposite surfaces of the membrane: $a_1 = a_2$, the linear in H terms in Eqs. 26 and 27 would cancel in the total free energy F :

$$F = \sum_{i=1,2} F_i = \sum_{i=1,2} N_i f_i \quad (29)$$

Nevertheless, as shown below, a linear in H term may arise when the up *vs* down symmetry of a membrane is broken, e.g. by applied pressure gradient in combination with the different boundary conditions at the monolayers peripheries, see Fig. 1.

To make the whole idea transparent we restrict our present derivation to the case of a "spherically homogeneous distributions" of molecules, i.e. considering a_i 's as being different for the different indices i 's, but position-independent within a curved part of the i -th monolayer. Below, we neglect the inhomogeneous distribution of the strain across the thickness of each monolayer. Also, we consider only spherical shapes of the curved part of the bilayer membrane, while introducing position independent (over the membrane's surface) mean and gaussian curvatures:

$$H = 1/r; \quad K = H^2 = 1/r^2 \quad (30)$$

where r is the radius of curvature. The radius of the base of the curved membrane is fixed at $R \leq r$, in accord with the fixed radius of the pipette, which sucks in the membrane, and creates a pressure difference P between inside and outside surfaces of the membrane in the experimental setup (Sukharev et al., 1999; Hase et al., 1995). Then, according to the Laplace's law we have:

$$T_1 + T_2 = Pr/2, \quad (31)$$

where T_i is the lateral tension in the i -th monolayer, and we neglected a small difference between the curvatures of the monolayers.

First, we consider the free energy of a flat, undeformed bilayer membrane, in order to use it as a reference value of the free energy per lipid molecule, f_0 . The flat membrane has a monolayer thickness $l_0 = v/a_0$, where the area per molecule a_0 is determined from the condition of the minimum of the free energy F defined in Eq. 29:

$$\partial F / \partial a_0 = 0, \quad \text{at:} \quad (32)$$

$$a_1 = a_2 = a_0, \quad H = K = 0, \quad N_1 = N_2 = N_0. \quad (33)$$

Using conditions from Eq. 33 in the Eqs. 22 - 29 we derive the following expression for the free energy per lipid molecule, f_0 , in the undeformed state:

$$f_0 = f_1(z_0, h = 0) = f_2(z_0, h = 0) = \epsilon_s z_0 + \epsilon_t \{1 + z_0^{-2} - 2z_0^{-1}\}, \quad (34)$$

where the following dimensionless parameters have been introduced:

$$z_i = a_i l_s / v; \quad h = l_s / r \equiv H l_s; \quad h_0 = l_s / R; \quad \epsilon_s = \gamma v / l_s; \quad \epsilon_t = k_s l_s^2 / 2. \quad (35)$$

It is useful for the comprehension of the rest of the paper to mention here orders of magnitude of the main parameters. Using the values of R and $l_s \sim l_0$ mentioned in the Introduction, we find that the dimensionless curvature is of the order: $h \sim 10^{-3} \ll 1$. Therefore, it could be inferred from Eqs. 23 and 24, and from the definition Eq. 25, that $v \approx l_s a_i$, which leads to an estimate: $z_i \sim 1$. The entropic nature of the f_{ti} term in Eq. 22 is reflected in the temperature dependent coefficient k_s , which for the known phospholipid bilayers is of the order (Ben-Shaul, 1995; Xiang and Anderson, 1994): $k_s l_s^2 \sim 25kT$, where k is the Boltzman's constant and T is the absolute temperature. The scale of the surface term f_{si} in Eq. 22 is characterized by the coefficient γ , which at room temperature is of the order (Ben-Shaul, 1995): $\gamma \sim 0.1kT/\text{\AA}^2$. Gathering all the estimates, and also taking into account that the typical value of an area per molecule is (Ben-Shaul, 1995): $a_i \sim 60\text{\AA}^2$, we obtain the following list of the estimates (taken for the room temperature $T \sim 300K$):

$$z_i \sim 1; \quad h \sim 10^{-3}; \quad \epsilon_s \sim 3 \cdot 10^{-13} \text{erg}; \quad \epsilon_t \sim 1.3\epsilon_s. \quad (36)$$

An additional important dimensionless parameter relates characteristic experimental value of the pressure difference $P \sim 50\text{mm Hg}$ (Sukharev et al., 1999; Hase et al., 1995) with the "microscopical bending energy" ϵ_t :

$$Pv/(2\epsilon_t) \sim 10^{-4} \quad \text{at:} \quad \epsilon_t \sim 5 \cdot 10^{-13} \text{erg}; \quad v \sim 1.2 \cdot 10^3 \text{\AA}^3, \quad (37)$$

where we use an estimate $l_s \sim 20\text{\AA}$ for the typical length of a free phospholipid molecule (Ben-Shaul, 1995) and $\epsilon_s = 0.6\epsilon_t$.

In the dimensionless parameters and variables equation Eq. 32 reads:

$$\partial f_0 / \partial z_0 = \epsilon_s + 2\epsilon_t \{z_0^{-2} - z_0^{-3}\} = 0, \quad (38)$$

or in the Cardano's form:

$$z_0^3 + p_0 z_0 + q = 0; \quad \text{where:} \quad p_0 = -q = 2\epsilon_t / \epsilon_s \quad (39)$$

$$\text{and:} \quad (q/2)^2 + (p_0/3)^3 \equiv (\epsilon_t / \epsilon_s)^2 + (2\epsilon_t / 3\epsilon_s)^3 > 0. \quad (40)$$

The inequality in Eq. 40 proves that there is a unique real root of the cubic equation Eq. 39. Solution z_0 depends only on the dimensionless parameter $p_0 \equiv 2\epsilon_t / \epsilon_s$. A numerical solution of Eq. 39 at $1/p_0 = 0.3$ gives:

$$z_0 = 0.829. \quad (41)$$

Substitution of the solution z_0 into Eq. 34 gives desired value of f_0 .

A. Free energy including patch and adhesion to the walls

The free energy expressions Eq. 22 and Eq. 29 do not account neither for the adhesion of some part of the upper monolayer to the wall of the pipette, nor for the existence of the patch, which serves as a reservoir of lipids for the lower monolayer, see Fig. 1. In order to include these features of the experimental setting (Sukharev et al., 1999; Hase et al., 1995) we write the total Helmholtz free energy of the membrane as follows:

$$F = N_1(f_1 - f_0) + N_2(f_2 - f_0 + E_{ad}) - N_1(a_1 - a_{01})T_1 - N_2(a_2 - a_{02})T_2 - (N_2 - N_{02})a_0 \sin \Theta \cdot (T_1 + T_2) - \sum_{i=1,2} \lambda_i(S_i(H) - N_i a_i). \quad (42)$$

Explain the right hand side (rhs) expression in Eq. 42 term by term. The first two terms signify the free energies of lipids in the curved parts of the monolayers 1 and 2 correspondingly. The energy per lipid molecule f_0 is subtracted in order to allow for the free energy difference between the molecules which belong to the curved part and to either the patch, or to the part of the monolayer 2 that is stuck to the wall of the pipette. In the latter case, we allow also for the adhesion, so that the energy per molecule is lowered with respect to the patch by an amount of the adhesion energy E_{ad} . The free energies per lipid molecule f_i in the i -th monolayer could be written using definitions Eqs. 22-29 and dimensionless variables Eq. 35 as follows:

$$f_1(z_1, h) \equiv \epsilon_s z_1 + \epsilon_t \left\{ (h^2/3)(7z_1^{-4} - 4z_1^{-3}) + 2h(z_1^{-2} - z_1^{-3}) + (z_1^{-1} - 1)^2 \right\}; \quad (43)$$

$$f_2(z_2, h) = f_1(z_2, -h). \quad (44)$$

The next two terms on the rhs of Eq. 42 represent a mechanical work done by the tensions $T_{i=1,2}$ by stretching an area per molecule in the curved part of the i -th monolayer from the initial to the final value, a_{0i} and a_i respectively. The initial areas a_{0i} , corresponding to the equilibrium state at zero external pressure gradient, are calculated below together with the initial numbers N_{0i} of the lipids in the curved parts of the monolayers. The fifth term on the rhs of Eq. 42 is introduced to allow for the mechanical work done by the perpendicular to the wall projections of the tensions during tearing off the 2nd monolayer from the pipette's wall. Angle Θ is the wetting angle between the membrane and the wall:

$$\sin \Theta = \{1 - \cos^2 \Theta\}^{1/2} = \{1 - (R/r)^2\}^{1/2} \equiv \{1 - (h/h_0)^2\}^{1/2}, \quad (45)$$

where notation defined in Eq. 35 is used. The factor $\sin \Theta \cdot (T_1 + T_2)$ in the fifth term signifies that the force acting on the 2nd monolayer perpendicular to the wall consists of the $\sin \Theta \cdot T_2$ projection added to the projection of $\sin \Theta \cdot T_1$, which is applied from the side of the 1st monolayer. The latter force equals, with an opposite sign, to the force acting perpendicular to the wall on the monolayer 1 in accord with the Newton's 3rd law. Next, the terms with the Lagrange multipliers $\lambda_{i=1,2}$ are introduced in order to select only the spherically shaped conformations of the membrane as its curvature H changes together with the external pressure.

In this case the external surface areas S_1 and S_2 of the monolayers and the numbers of the molecules in them are related by the following equations:

$$S_1(H) = 2\pi(r - l_1)^2 \left(1 - \{1 - R^2/(r - l_1)^2\}^{1/2}\right) = N_1 a_1 ; \quad (46)$$

$$S_2(H) = 2\pi(r + l_2)^2 \left(1 - \{1 - R^2/(r + l_2)^2\}^{1/2}\right) = N_2 a_2 . \quad (47)$$

Here the thicknesses $l_{i=1,2}$ of the i -th monolayer are defined in Eqs. 23 and 24. As long as the ratios are small:

$$l_i/r \leq l_i/R \sim 10^{-3} , \quad (48)$$

we shall neglect small corrections l_i to the curvature radius r in the expressions in Eqs. 46 and 47, hence defining a unique surface area function $S(H)$:

$$S(H) = 2\pi r^2 \left(1 - \{1 - R^2/r^2\}^{1/2}\right) \equiv 2\pi H^{-2} \left(1 - \{1 - (HR)^2\}^{1/2}\right) \quad (49)$$

Then, using Eq. 49 and relations Eq. 46, Eq. 47, together with definitions Eq. 35 we express the number of the lipids in the flat bilayer N_0 as follows:

$$S_0 = S(H \rightarrow 0) = \pi R^2 = N_0 a_0 = N_0 z_0 v / l_s . \quad (50)$$

B. Equilibrium conformation under zero external pressure difference: $P = 0$

In the absence of pressure, the membrane is essentially flat, subjected to the "resting" (Sukharev et al., 2001) tension arising from the membrane adhesion to the (glassy) surface of the pipette. Thus, consider first a bilayer membrane in the equilibrium state in the pipette before an external pressure gradient is applied. Then, the tensions induced according to the Laplace's law Eq. 31 by the external pressure difference P are zero:

$$T_1 = T_2 = 0 , \quad (51)$$

and the free energy equals:

$$F = N_{01}(f_1 - f_0) + N_{02}(f_2 - f_0 + E_{ad}) - \sum_{i=1,2} \lambda_i (S(H) - N_{0i} a_{0i}) . \quad (52)$$

Corresponding equilibrium equations minimizing F in Eq. (52) are derived in Appendix. Using also relations Eq. 46 and Eq. 47, we obtain the following closed form equation for the unknown value of H expressed in the dimensionless variable h defined in Eq. 35:

$$\sum_{i=1,2} n_i \partial f_i / \partial h = -(1/N_0) (\partial S(h) / \partial h) \sum_{i=1,2} \partial f_i / \partial z_i ; \quad (53)$$

$$\text{where: } n_i \equiv N_i / N_0 = 2(z_0 / z_i) (h_0 / h)^2 \left(1 - \{1 - (h/h_0)^2\}^{1/2}\right) . \quad (54)$$

The functions f_i are defined in Eqs. 43 and 44.

C. Semi-equilibrium conformation at finite external pressure difference P

Soon after an application of a finite external pressure difference P perpendicular to the plane of the membrane, i.e. during the times $\Delta t \leq t \ll \tau_s$, a semi-equilibrium conformation is achieved. The free energy of the membrane in the semi-equilibrium state could be written using Eq. 42 as follows:

$$F \rightarrow F - \lambda_3(N_1 - N_2 - N_{01} + N_{02}). \quad (55)$$

Hence:

$$F = N_1(f_1 - f_0) + N_2(f_2 - f_0 + E_{ad}) - (N_2 - N_{02})a_0 \sin \Theta \cdot (T_1 + T_2) - \sum_{i=1,2} [N_i(a_i - a_{0i})T_i + \lambda_i(S_i(H) - N_i a_i)] - \lambda_3(N_1 - N_2 - N_{01} + N_{02}). \quad (56)$$

Here an extra Lagrange multiplier λ_3 is introduced to reflect a simple physics. Namely, as explained in the Introduction, we consider the semi-equilibrium state as existing during such a short time, which is not enough for a transfer of the lipid molecules from the patch to the curved part of the monolayer 1. Hence, a change of the numbers of lipids $N_i(P) - N_{i0}$, in the curved parts of the monolayers $i = 1, 2$ relative to the initial, $P = 0$ equilibrium conformation occurs only due to a tearing off the 2nd monolayer from the pipette's wall. In the latter case it is reasonable to assume that the numbers of lipids in both monolayers increase simultaneously by the same amount (no interlayer slide):

$$N_1 - N_{01} = N_2 - N_{02}. \quad (57)$$

Here N_{0i} are involved, which had to be found from the Eqs. A1-A4. Condition Eq. 57 is maintained by the term with λ_3 in Eq. 56. As explained in the Introduction, due to small thickness of the membrane Eq. 48 we assume equal lateral tensions in the monolayers, which then could be found from the Laplace relation Eq. 31:

$$T_1 = T_2 = Pr/4 \equiv T/2, \quad (58)$$

Here new parameter T is introduced for convenience. Corresponding equations for the minimum of Eq. 56 are presented in the Appendix.

D. Relaxed conformation at finite external pressure difference P

Equations for a complete (relaxed) equilibrium conformation of the membrane are readily obtained, see Appendix, starting from the following expression for the free energy:

$$F = N_1(f_1 - f_0) + N_2(f_2 - f_0 + E_{ad}) - (N_2 - N_{02})a_0 T \sin \Theta - N_2(a_2 - a_{02})T - \sum_{i=1,2} \lambda_i(S_i(H) - N_i a_i). \quad (59)$$

Equation 59 is obtained from Eq. 56 by "relaxing" to zero the tension T_1 in the monolayer 1, and by dismissing a condition of a "dynamic cut off" of the first monolayer from the reservoir of lipid molecules, i.e. from the patch. The latter condition was represented in Eq. 56 by the term with the Lagrange multiplier λ_3 . The lateral tension in the monolayer 2 obeys the following Laplace relation:

$$T_2 = Pr/2 \equiv T \quad ; T_1 = 0. \quad (60)$$

Corresponding equations for the minimum of Eq. 59 are presented in the Appendix.

IV. DISCUSSION OF NUMERICAL RESULTS

A. Initial equilibrium state

Results obtained by the numerical solution of equations A1-A4 are represented in Table 1. Despite the absence of the external pressure gradient: $P = 0$, the curvature $1/r$ proves to be small but finite: $R/r \sim 10^{-3}$. This happens due to finite adhesion energy E_{ad} of the monolayer 2 to the wall of the pipette. In Table 1 n_2 is the number of molecules in the curved part of the monolayer 2 normalized with the number N_0 in a free monolayer. Presented data indicate that n_2 decreases with an increase of the adhesion energy E_{ad} . The relative decrease of n_2 ranges from 0.8% at $E_{ad}/\epsilon_t = 0.03$ to 9% at $E_{ad}/\epsilon_t = 0.3$. Simultaneously, the relative number of molecules n_1 ($n_1 = N_1/N_0$) in the monolayer 1 remains practically constant and equals 1. The reason for the different behaviour of n_1 and n_2 is obvious. More molecules from the curved part of the monolayer 2 tend to stick to the wall as the adhesion energy E_{ad} increases. On the other hand, though the monolayer 1 leans to the wall following the shape of the monolayer 2, it does not stick, hence it compensates for the "losses" of the number of molecules in its curved part by absorbing extra molecules from the patch.

Table 1 also contains the values of the areas $a_{1,2}$ per molecule in the monolayers, expressed in dimensionless units via the variables z_1, z_2 defined in Eq. 35. The range of E_{ad}/ϵ_t is chosen from the consideration of the stability of the membrane under stretching of its area, which is known to have an upper threshold (Sukharev et al., 1999) of about $(a_i - a_0)/a_0 \approx 4\%$. Remarkable is that in this way our theory predicts reasonably well the value of the adhesion line tension T_a of a lipid membrane to the glass wall known from the experiment (Opsahl and Webb, 1994). Indeed, theoretically chosen ratio $E_{ad}/\epsilon_t = 0.03$ in combination with experimentally known absolute values $\epsilon_t \sim 4 \cdot 10^{-13} \text{ erg}$ and $a_0 \sim 60 \text{ \AA}^2$ leads to the estimate :

$$T_a \sim E_{ad}/a_0 = 2.5 \text{ dyn/cm}, \quad (61)$$

which falls right inside the experimentally measured interval $T_a = 0.5 \div 4 \text{ dyn/cm}$ (Opsahl and Webb, 1994).

Finally, the last line of Table 1 provides normalized values of the free energy of the membrane F , defined in Eq. 52. It is interesting to notice that the values of $F/(N_0\epsilon_t)$ practically coincide with the corresponding values of the (normalized) adhesion energy per molecule E_{ad}/ϵ_t , which are also indicated in Table 1. An examination of Eq. 52 leads to the conclusion that the coincidence is not accidental. Namely, while the reference of energy for the molecules in the monolayer 1 is approximately f_0 per molecule, the one for the monolayer 2 is $f_0 - E_{ad}$. At zero external pressure $P = 0$ the free energy per molecule in each monolayer approximately equals f_0 , i.e. the flat membrane's value. Therefore, contribution of the monolayer 1 to F in Eq. 52 is nearly zero, and contribution of the monolayer 2 is indeed $\approx E_{ad}N_0$, as long as $N_{02} \approx N_0$.

B. Conformations at $P \neq 0$

Numerical results were obtained by minimizing the free energy expressions of the membrane in the pipette under a fixed external pressure. Expressions Eq. 56 and Eq. 59 were used, describing correspondingly the semi- and complete equilibrium states of the membrane. The calculated theoretical dependences are presented in Figs. 2, and 3. Based on the experimental data (Sukharev et al., 1999; Hase et al., 1995; Sukharev et al., 2001) we had chosen the following values for the two dimensionless ratios controlling the main dependences:

$$\epsilon_s/\epsilon_t = 0.6; \quad E_{ad}/\epsilon_t = 0.03. \quad (62)$$

The first ratio in Eq. 62 sets the scale of the surface tension, while the second ratio fixes the scale of the adhesion energy of the membrane to the glassy wall of the pipette with respect to the energy of the entropic repulsion between the hydrocarbon tails in the depth of each monolayer.

As is shown in Fig. 2a, the free energy of the relaxed conformation is lower than that one in the semi-equilibrium state at any pressure difference P measured in the dimensionless units introduced in Eq. 37:

$$P \rightarrow p \equiv Pv/(2\epsilon_t). \quad (63)$$

The Fig. 2a justifies our conjecture made in the Introduction that a relaxation to zero of the lateral tension T_1 in the concave monolayer 1 is concomitant with the decrease of the free energy F of the bilayer membrane kept at a fixed external pressure difference. A slide of the monolayer 2 is prevented by its finite adhesion energy to the wall of the pipette, i.e. E_{ad} .

Next, Fig. 2b provides an important evidence that the decrease of the free energy and vanishing of T_1 happens by virtue of an increase of the number of lipid molecules in the curved part of the monolayer 1 at a constant pressure difference P . Indeed, n_1^{conn} is manifestly greater than n_1^{disc} at the same pressure. Simultaneously, n_2^{conn} is even slightly smaller than n_2^{disc} . The increase of n_2 under fast growth of the external pressure P happens due to a tearing off the membrane from the glassy wall of the pipette. In the absence of the transfer of lipids from the

patch, an "instant" increase of n_1^{disc} with pressure in the semi-equilibrium state follows that one of n_2^{disc} and has the same origin, i.e. tearing off the membrane from the wall. But, after enough time had elapsed since the beginning of the pressure pulse, the n_1 shows an increase from n_1^{disc} up to n_1^{conn} at a fixed pressure due to a transfer of lipids from the patch. The latter effect happens either via interlayer slide or/and via lipid diffusion, as discussed in the Introduction. During this relaxation process the area per molecule in the monolayer 1 decreases from z_1^{disc} (in the dimensionless units) to practically that one in the free bilayer: $z_1^{conn} \approx z_0$, see Fig. 3a. Simultaneously, the monolayer 2 has to bear now the whole lateral tension: $T_2 = T$; $T_1 = 0$ (previously shared with the monolayer 1: $T_2 = T_1 = T/2$). The area per molecule in the monolayer 2 stretches from z_2^{disc} to z_2^{conn} . As long as an increase of this area relative to a free bilayer value exceeds $4 \div 5\%$ the membrane becomes unstable. Therefore, we deduce from Fig. 3a, that the range of the external pressure differences in our model should be bound as follows: $0 \leq P \leq 1.5$.

Results of our calculations of the membrane's curvature as a function of the pressure P are presented in Fig. 2c. There is apparent effective softening of the membrane after a relaxation at constant P , i.e. $h_{conn} > h_{disc}$. Also, the curves exhibit tendency to a saturation of the curvature at high enough pressures, in a qualitative accord with the experimental data (Sukharev et al., 1999). Nevertheless, according to our results plotted in Fig. 3b, the lateral tension T_1 continues to grow smoothly as a function of pressure P even in the region of (near) saturation of the curvature.

Finally, we mention here, that separate consideration of the semi- and complete equilibrium states discussed above, is justified by the fact that the characteristic stress relaxation time: $\tau_{s,d} \sim 0.1 \div 1 sec$ differs by $4 \div 5$ orders of magnitude from the characteristic time Δt necessary for a propagation of the bending deformations over a membrane with the linear dimensions $R \sim 1 \mu m$:

$$\Delta t \sim R^2 (\rho l_0 / \epsilon_t)^{1/2} \sim 10^{-8} cm^2 \left(1g/cm^3 \cdot 10^{-7} cm / 10^{-13} erg \right)^{1/2} \sim 10^{-5} sec. \quad (64)$$

Here we used a well known formula for the frequency of the bending waves in a thin plate (Landau and Lifshitz, 1980):

$$\omega_b = q^2 \{k_B / (2l_0\rho)\}^{1/2}, \quad (65)$$

where k_B is the bending modulus, q is a wave-vector, ρ is the mass density of the membrane, and $2l_0$ is its thickness. Actually, the latter is dynamically increased by a drag of the adjacent layers of the liquid in which the membrane is immersed. In Eq. 64 we use ϵ_t as an estimate of k_B involved in Eq. 65 allowing for the role played by ϵ_t as a bending coefficient. This is justified by a direct comparison of the free energy expressions Eqs. 26, 27 and the definition of ϵ_t given in Eq. 35.

V. SUMMARY

Dynamics and characteristic times of bilayer membrane with MscL channels in the patch-clamp experimental setting are studied theoretically. The different

characteristic times range from $10^{-5} \div 10^{-4} \text{ sec}$ to several seconds. The shortest time corresponds to stress propagation along the micrometer-sized membrane bent by external pressure gradient. The external pressure produces lateral tension in the bilayer, which opens mechanosensitive channels (MscL). We show that lateral tension in lipid bilayer does not remain constant under constant pressure gradient applied to the membrane. Interlayer slide leads to redistribution of lateral stress within $0.01 \div 0.1 \text{ sec}$ after application of the pressure step. Relaxation of lateral stress in the lower monolayer triggers closing back of MscL channels ("adaptation"), observed experimentally, see companion paper. The longest time ($\sim 1 \text{ sec}$) arises from the free energy barrier for the transition from the open to the closed MscL conformation.

We have analysed the influence of bilayer hydrophobic thickness on the hydrophobic mismatch energy and MscL thermodynamics. Thick bilayer hinders MscL opening, while thin bilayer favours the open conformation of the channels. Our estimates of the mismatch energy give values in the range $2 \div 20 k_B T_0$, where $k_B T_0$ is the thermal energy at room temperature T_0 . This estimate is comparable with the free energies in the MscL elastic model (Sukharev et al., 1999) and (Sukharev and Markin, 2001). Depending on the bilayer thickness, the hydrophobic mismatch favours either closed or open MscL conformation, as outlined in Section II. This may explain why MscL adaptation phenomenon, being present in the PC-20 lipid bilayers, is absent in the PC-18 bilayers (see companion paper).

We have studied the free energy functional of the membrane modeling the patch-clamp experimental setting. Minimizing the free energy functional, we have found parameters of the membrane conformation as function of pressure gradient for two (semi- and complete) equilibrium states. The semi-equilibrium state is an instantaneous mechanical equilibrium state achieved after application of external pressure step to the membrane. Following it, a transfer of lipid molecules along the lower monolayer (see Fig. 1) takes place. It leads to the leveling of the finite lateral tension in the strained part of the lower monolayer with zero tension existing in the outer patch. As a result the free energy reaches its true minimum and the membrane achieves the complete equilibrium state. The upper monolayer is fixed due to lipid adhesion to the pipette glass wall. Our free energy functional of the membrane includes this adhesion energy. Theoretically predicted value of the adhesion line tension in our model is in a good agreement with experimental data (Opsahl and Webb, 1994).

The transfer of lipids in the lower monolayer may occur either via interlayer slide or/and via diffusion of lipids into the stretched region of the lower monolayer from the outer patch (see Fig. 1), see also (Baoukina and Mukhin, 2003) and (Mukhin and Baoukina, 2002. Lipids diffusion mechanism of stress relaxation in a bilayer fluid membrane under pressure. cond-mat/0206099). Characteristic time of the individual lipid diffusion processes is by one order of magnitude longer than the time of the interlayer slide (collective motion of the lipids constituting the lower monolayer). Nevertheless, this times may become comparable at high enough density of MscL's, which then would pin the monolayer against slide.

The above explanation of the slide-triggered closing of a MscL leads to a

proposal (Th. Schmidt, Leiden University, personal communication, 2002) of a possible experimental check up of the theory. Namely, suppose that the membrane with MscL has been turned over, so that the cytoplasmic half of the channel belongs now to the monolayer 2, which in turn sticks to the wall of the pipette. Then, the opening of the channel would be controlled by the lateral tension T_2 , which does not vanish (it even increases) after the relaxation of the membrane under a constant pressure. Hence, one would expect that adaptation of MscL after an application of the opening pressure would be less probable in this case.

Finally, we mention some possible future improvements of the theory. These could be made by lifting the simplifying restrictions of the homogeneity of the lateral stresses (tensions) across the thickness of each monolayer. Besides, one may abandon the approximation of a position-independent area per molecule on the membrane's surfaces. As a consequence, in a more elaborate scheme of derivations one would not restrict himself to the spherical symmetry of the membrane's shape. Nevertheless, we believe that these improvements would not deny the main physical concepts considered in this paper.

The authors are grateful to S.I. Sukharev for the introduction in the problem and for numerous enlightening discussions during the work. Useful discussions with Jan Zaanen and comments by R.F. Bruinsma and Th. Schmidt are highly acknowledged.

REFERENCES

- Baoukina S.V. and S.I. Mukhin. 2003. Inter-layer slide mechanism of stress relaxation in bilayer fluid membrane under pressure. *Biophys. J.* 84: 1129a.
- Ben-Shaul A. 1995. Molecular theory of chain packing, elasticity and lipid-protein interaction in lipid bilayers. *In* Structure and Dynamics of membranes. Elsevier Science., 359-401
- Betanzos Monica, Chien-Sung Chiang, H. Robert Guy and Sergei Sukharev. 2002. A large iris-like expansion of a mechanosensitive channel protein induced by membrane tension. *Nature Structural Biology* 9: 704-710
- Cantor R.S. 1999. Lipid composition and the lateral pressure profile in bilayers. *Biophys. J.* 76: 2625-2639
- Doyle D.A., J.M. Cabral, R.A. Pfuetzner, A. Kuo, J.M. Gulbis, S.L. Cohen, B.T. Chait, R. MacKinnon. 1998. The structure of the potassium channel: molecular basis of K⁺ conduction and selectivity. *Science.* 280:69-77
- Fournier J.-B. 1999. Microscopic membrane elasticity and interactions among membrane inclusions: interplay between the shape, dilation, tilt and tilt-difference modes. *Eur. Phys. J.* 11:261-272
- Gullingsrud J., K. Schulten. 2003. Gating of MscL studied by steered molecular dynamics. *Biophys. J. Supplement* 84: 21a
- Hamill O.P. and B. Martinac. 2001. Molecular basis of mechanotransduction in living cells. *Physiol. Rev.* 81: 685-740
- Hase C.C., A.C. Le Dain, B. Martinac. 1995. Purification and functional reconstitution of the recombinant large mechanosensitive ion channel of *Escherichia coli*. *J. Biol. Chem.* 270:18329-18334
- Jian-Guo H., O.Y. Zhong-Can. 1993. Shape equations of the axisymmetric vesicles. *Phys. Rev. E* 47: 461-467
- Landau L.D., E.M. Lifshitz 1980. Theory of Elasticity. V.7. Theoretical Physics. Pergamon Press, New York
- Liu Q.H., H.G. Zhou, J.X. Liu, O.Y. Zhong-Can. 1999. Spheres and prolate and oblate ellipsoids from an analytical solution of spontaneous curvature fluid membrane model. *Phys. Rev. E* 60:3227-3233
- Ming Zhou, J.H. Morais-Cabral, S. Mann, R. MacKinnon. 2001. Potassium channel receptor site for the inactivation gate and quaternary amine inhibitors. *Nature.* 411:657-661
- Opsahl L.R., W.W. Webb. 1994. Lipid-glass adhesion in giga-sealed patch-clamped membranes. *Biophys. J.* 66: 75-79
- Sachs F. and C.E. Morris. 1998. Mechanosensitive ion channels in nonspecialized cells. *Revs. Physiol. Biochem. Pharmacol.* 132: 1-77
- Safran S.A. 1994. Statistical thermodynamics of surfaces, interfaces and membranes. *In* Frontiers in Physics, Vol. 90. Perseus Pr. Publisher
- Sonnleitner A., G.J. Schultz, and Th. Schmidt. 1999. Free Brownian motion of individual lipid molecules in biomembranes. *Biophys. J.* 77: 2638-2642
- Sukharev S.I., W.J. Sigurdson, C. Kung, F. Sachs. 1999. Energetic and spatial parameters for gating of the bacteria large conductance mechanosensitive

- channel. *J. Gen. Physiol.* 113:525-539
- Sukharev S., M. Betanzos, C.S. Chiang, H.R. Guy. 2001. The gating mechanism of the large mechanosensitive channel MscL. *Nature.* 409:720-724
- Sukharev S.I. and V.S. Markin. 2001. Kinetic model of the bacterial large conductance mechanosensitive channel. *Biological membranes* 18:440-445
- Xiang T.X., B.D. Anderson. 1994. Molecular distributions in interphases: statistical mechanical theory combined with molecular dynamics simulation of a model lipid bilayer. *Biophys. J.* 66:561-573
- Zhong-Can O.Y., W. Helfrich. 1987. Instability and deformation of a spherical vesicle by pressure. *Phys. Rev. Lett.* 59:2486-2488
- Zhong-Can O.Y., W. Helfrich. 1989. Bending energy of vesicle membranes. *Phys. Rev. A* 39:5280-5288

APPENDIX A: EQUILIBRIUM EQUATIONS

1. Equilibrium conformation, $P = 0$

Considering N_{0i} , a_{0i} and H as the five independent variables, we minimize F in Eq. (52) with respect to all of them, and thus obtain the following equilibrium equations:

$$\partial F/\partial N_{01} = 0 : \quad \{f_1 - f_0\}/a_{01} = -\lambda_1 ; \quad (\text{A1})$$

$$\partial F/\partial N_{02} = 0 : \quad \{f_2 - f_0 + E_{ad}\}/a_{02} = -\lambda_2 ; \quad (\text{A2})$$

$$\partial F/\partial a_{0i} = 0 : \quad \partial f_i/\partial a_{0i} = -\lambda_i , i = 1, 2 ; \quad (\text{A3})$$

$$\partial F/\partial H = 0 : \quad \sum_{i=1,2} N_{0i} \partial f_i/\partial H = (\lambda_1 + \lambda_2) \partial S(H)/\partial H . \quad (\text{A4})$$

One can easily see that Eqs. A1 and A2 permit exclusion of the Lagrange multipliers λ_i from the equations A3 and A4. Then, solving Eq. A3 for $i = 1, 2$ we find dependences $a_{0i}(H)$, and substitute them into Eq. A4. In accord with the discussion at the beginning of the Section III, after Eq. (42), the Lagrange multiplier λ_2 in Eq. A3 plays a role of the "resting" tension in the layer 2 due to a finite adhesion energy E_{ad} of the layer to the glassy wall of the pipette.

2. Semi-equilibrium conformation, $P \neq 0$

In order to find the minimum of (56) we consider N_{0i} , a_{0i} and H as the five independent variables. Hence, we minimize F with respect to all of them, and thus obtain the following equilibrium equations:

$$\partial F/\partial N_1 = 0 : \quad f_1 - f_0 - (T/2)(a_1 - a_{01}) - (T/2)a_0 \sin \Theta = \lambda_3 - \lambda_1 a_1 ; \quad (\text{A5a})$$

$$\begin{aligned} \partial F/\partial N_2 = 0 : \quad & f_2 - f_0 + E_{ad} - (T/2)(a_2 - a_{02}) - (T/2)a_0 \sin \Theta = \\ & -\lambda_3 - \lambda_2 a_2 ; \end{aligned} \quad (\text{A5b})$$

$$\partial F/\partial a_i = 0 : \quad \partial f_i/\partial a_i - T/2 = -\lambda_i , i = 1, 2 ; \quad (\text{A5c})$$

$$\begin{aligned} \partial F/\partial H = 0 : \quad & \sum_{i=1,2} N_i [\partial f_i/\partial H - \partial(T/2)/\partial H (a_i - a_{0i})] - \\ & a_0 (N_2 - N_{02}) \partial(T \sin \Theta)/\partial H = (\lambda_1 + \lambda_2) \partial S(H)/\partial H . \end{aligned} \quad (\text{A5d})$$

The system of equations Eqs. A5a-A5d is solved numerically under condition Eq. 57, after making a transformation to the dimensionless variables Eq. 35 and after normalization of the numbers N_i by N_0 in accord with Eq. 54.

3. Equilibrium (relaxed) conformation, $P \neq 0$

Equations minimizing the free energy F in Eq. 59 take the form:

$$\partial F/\partial N_1 = 0 : f_1 - f_0 = -\lambda_1 a_1 ; \quad (\text{A6a})$$

$$\partial F/\partial N_2 = 0 : f_2 - f_0 + E_{ad} - T(a_2 - a_{02}) - T a_0 \sin \Theta = -\lambda_2 a_2 ; \quad (\text{A6b})$$

$$\partial F/\partial a_1 = 0 : \partial f_1/\partial a_1 = -\lambda_1 ; \quad (\text{A6c})$$

$$\partial F/\partial a_2 = 0 : \partial f_2/\partial a_2 - T = -\lambda_2 ; \quad (\text{A6d})$$

$$\begin{aligned} \partial F/\partial H = 0 : \sum_{i=1,2} N_i \partial f_i/\partial H - N_2 (\partial T/\partial H)(a_2 - a_{02}) - \\ a_0 (N_2 - N_{02}) \partial (T \sin \Theta)/\partial H = (\lambda_1 + \lambda_2) \partial S(H)/\partial H . \end{aligned} \quad (\text{A6e})$$

The system of equations Eqs. A6a-A6e is solved numerically after making a transformation to the dimensionless variables Eq. 35 and Eq. 54.

APPENDIX B: ELASTIC MODEL OF MSCL CHANNEL

1. Phenomenological theory

We consider a simple phenomenological model of MscL channel (Sukharev, Markin, 2001). The channel is presented as elastic cylinder; it's stiffness is different in closed and open conformations. The free energy of the closed channel, F_C , is written as:

$$F_C = \frac{B_C}{2} (A - A_C)^2 - T(A - A_C), \quad (\text{B1})$$

here B_C is elastic modulus of the channel in the closed conformation; T - tension transmitted through the lipid bilayer; A_C - is the cross-section area of the closed channel in the absence of tension in lipid bilayer; A - is the channel cross-section area at a given tension T . Transition to the open conformation of the channel is associated with stretching the channel area, rearrangement of transmembrane domains (helices) (Sukharev et al., 2001), (Gullingsrud and Schulten, 2003) and requires additional work. The work of opening the channel is done by tension in lipid bilayer. The free energy of the channel in the open state, F_O , equals:

$$F_O = \frac{B_O}{2} (A - A_O)^2 + E_O - T(A - A_C), \quad (\text{B2})$$

here B_O - elastic modulus of the open channel ($B_O \gg B_C$); A_O - the area of open channel at zero tension ($A_O > A_C$); E_O - the (free) energy difference between open and closed conformations of the channel at zero tension in the bilayer. The finite energy E_O reflects the fact that the probabilities to find the channel in the open or closed states (P_O or P_C) are not equal (at zero tension the MscL is closed). In general, the value of E_O depends on many factors, e.g. the type of lipids in the bilayer, thermodynamic conditions of the surrounding solution, and also on the hydrophobic mismatch energy, F_{LP} (Hamill and Martinac, 2001). The latter is different for open and closed conformations of the channel, because MscL opening is associated with decrease of it's hydrophobic thickness (S. Sukharev, Maryland University, personal communication, 2003). For the given (open or

closed) state of the MscL channel, F_{LP} contributes to the total free energy of this conformation (F_O or F_C) and thus defines the value of E_O . At tension T the minima of the parabolas F_C and F_O define the free energies of the closed and open states, and the corresponding areas, A_C^T or, A_O^T are the areas occupied by closed or open channel in equilibrium:

$$A_C^T = \frac{T}{B} + A_C, \quad A_O^T = \frac{T}{B} + A_O, \quad (\text{B3})$$

$$F_C(A_C^T) = -\frac{T^2}{2B_C}, \quad F_O(A_O^T) = -\frac{T^2}{2B_O} - T(A_O - A_C) + E_O. \quad (\text{B4})$$

The equilibrium distribution of open/closed channels, n_O/n_C , at a given tension in membrane depends on the energy difference between open and closed conformations of the channel, $F_O - F_C$:

$$\frac{n_O}{n_C} = \frac{P_O}{P_C} \sim \exp\{-(F_O - F_C)/k_B T_0\}, \quad (\text{B5})$$

here n_O and n_C are fractions of open and closed channels, respectively; k_B - Boltzmann constant; T - temperature. The intersection point of the energy parabolas $F_C(A)$ and $F_O(A)$ is the barrier energy for transition between closed and open states, $F_{bar}(A_b)$:

$$F_C(A_b) = F_O(A_b) = F_{bar}(A_b). \quad (\text{B6})$$

By comparing (B1) and (B2), one finds that the area A_b ($A_C < A_b < A_O$) does not depend on the tension, T . The activation energies for closing and opening of the channel, $E_{act,c}$ and $E_{act,o}$:

$$E_{act,c} = F_{bar}(A_b) - F_O(A_O^T), \quad E_{act,o} = F_{bar}(A_b) - F_C(A_C^T) \quad (\text{B7})$$

define the kinetics of transitions between closed and open states. The activation barriers for closing and opening of the channel equal:

$$E_{act,c} = F_{bar}(A_b) - F_O(A_O^T) = \frac{B_O}{2}(A_O - A_b)^2 + T(A_O - A_b) + \frac{T^2}{2B_O}; \quad (\text{B8})$$

$$E_{act,o}(T) = \frac{B_0}{2}(A_b - A_C)^2 - T(A_b - A_C) + \frac{T^2}{2B_C}. \quad (\text{B9})$$

Solving Eq. (B6) with respect to A_b and substituting the result into Eq. (B8), one finds dependence $E_{act,c}$ on E_0 , shown in Fig. 5 for the different values of the tension T . As could be discerned already in Fig. 4, $E_{act,c}$ decreases with the increase of E_0 .

The equilibrium distribution of closed and open channels (B5) is reached within the characteristic time τ_{eqv} :

$$\tau_{eqv} = (k_O + k_C)^{-1}, \quad (\text{B10})$$

here k_O and k_C are the rates of opening and closing of the channels. The value of the rate constant for the open to closed transition, k_C , is the key factor for the channel closing induced by interlayer slide (as $n_C \rightarrow 1$):

$$k_C = \tilde{k} \exp\{-E_{act,c}/k_B T_0\}. \quad (\text{B11})$$

2. The energy of hydrophobic mismatch

The mismatch of hydrophobic thickness of the protein and that of the surrounding lipid bilayer makes lipids adjust to the protein length. This induces local deformation of lipid molecules. The deformation profile, $d(r)$, can be presented in a simple exponential form (Ben-Shaul, 1995):

$$d(r) = d_0 + (d_p - d_0) \exp \{-(r - r_p)/r_0\}, \quad (\text{B12})$$

here: r -distance from the protein center in the membrane plane; r_p -radius of the protein (protein is modeled as a cylinder); d_0 - the (equilibrium) thickness of the bilayer hydrophobic core in the absence of protein; d_p - is the thickness of protein's hydrophobic region; r_0 - the characteristic scale of the deformation. For the sake of simplicity let us consider a flat bilayer. The energy (per unit area) of elastic deformation of the bilayer by a cylindrical protein, f_{LP} , to the lowest order (neglecting tilt of lipid chains) can be written as (Fournier, 1999):

$$f_{LP} = \frac{K_d}{2}(d - d_0)^2 + \frac{K_g}{2}(\nabla d)^2, \quad (\text{B13})$$

here K_d is the dilation modulus, $K_d \sim 2K_A/(2l_0)^2$; K_g - is the modulus, characterizing the energy cost of producing a gradient of bilayer thickness (it includes the energy of increasing the area of chain-water interface (Fournier, 1999)).

We consider the concentration of the proteins to be small and calculate the hydrophobic mismatch energy, F_{LP} , per channel as follows:

$$F_{LP} = \int_{r_p}^{\infty} f_{LP} 2\pi r dr. \quad (\text{B14})$$

The result of the integration is:

$$F_{LP} = \frac{\pi}{4}(K_d r_0^2 + K_g) \left(\frac{2r_p}{r_0} + 1 \right) (d_p - d_0)^2. \quad (\text{B15})$$

Assuming $K_d \sim 15 \cdot 10^{14} \text{ erg/cm}^4$ (Hamill and Martinac, 2001), $K_g \sim 35 \text{ erg/cm}^2$ (Fournier, 1999), $r_0 \approx 10 \text{ \AA}$ (Ben-Shaul, 1995), $r_p \approx 25 \text{ \AA}$ (Sukharev et al., 1999), we obtain the following estimates for F_{LP} for two different values of hydrophobic mismatch, $d_p - d_0$:

1) for $|d_p - d_0| \sim 2 \text{ \AA}$, $F_{LP} \sim 2.3 k_B T_0$ at room temperature T_0 ;

2) for $|d_p - d_0| \sim 6 \text{ \AA}$, $F_{LP} \sim 21 k_B T_0$;

here k_B is the Boltzmann constant, T_0 is temperature. The value of $d_p - d_0$ depends on the type of lipids (i.e. the length of hydrocarbon chains) and on the state of the protein channel.

TABLES

TABLE I. Numerical results: initial equilibrium at $P = 0$

$E_{ad}/\epsilon_t = 0.03$	$E_{ad}/\epsilon_t = 0.06$	$E_{ad}/\epsilon_t = 0.1$	$E_{ad}/\epsilon_t = 0.3$
$z_2/z_0 = 1.0077$	$z_2/z_0 = 1.0158$	$z_2/z_0 = 1.027$	$z_2/z_0 = 1.093$
$n_2 = 0.9923$	$n_2 = 0.9844$	$n_2 = 0.9737$	$n_2 = 0.9151$
$F/(N_0\epsilon_t) = 0.03$	$F/(N_0\epsilon_t) = 0.0596$	$F/(N_0\epsilon_t) = 0.0988$	$F/(N_0\epsilon_t) = 0.2878$
$z_1 = z_0 = 0.8291,$	$n_1 = 1.000$	for all values of	$E_{ad}/\epsilon_t.$

Figure Legends

Fig. 1. Sketch of a membrane in the experimental patch-clamp settings. The numbering 1,2 of the monolayers within a bilayer membrane is indicated.

Fig. 2*a*. Normalized free energy $F/(\epsilon_t N_0)$ in the semi-equilibrium F_{disc} and complete equilibrium F_{conn} state *versus* dimensionless pressure difference p (see Eq. 63); $\epsilon_s/\epsilon_t = 0.6$.

Fig. 2*b*. Normalized numbers of lipid molecules in the curved parts of the membrane monolayers $n_{i=1,2}$ in the semi-equilibrium n_i^{disc} and complete equilibrium n_i^{conn} state (see Eq. 54) *versus* dimensionless pressure difference p . Other parameters are as in Fig. 2*a*.

Fig. 2*c*. Normalized curvature of the bilayer membrane inside the pipette in the semi-equilibrium h_{disc}/h_0 and complete equilibrium h_{conn}/h_0 state *versus* dimensionless pressure difference p ; $h/h_0 \equiv R/r$, where R and r are the pipette and the curvature radii respectively. Other parameters are as in Fig. 2*a*.

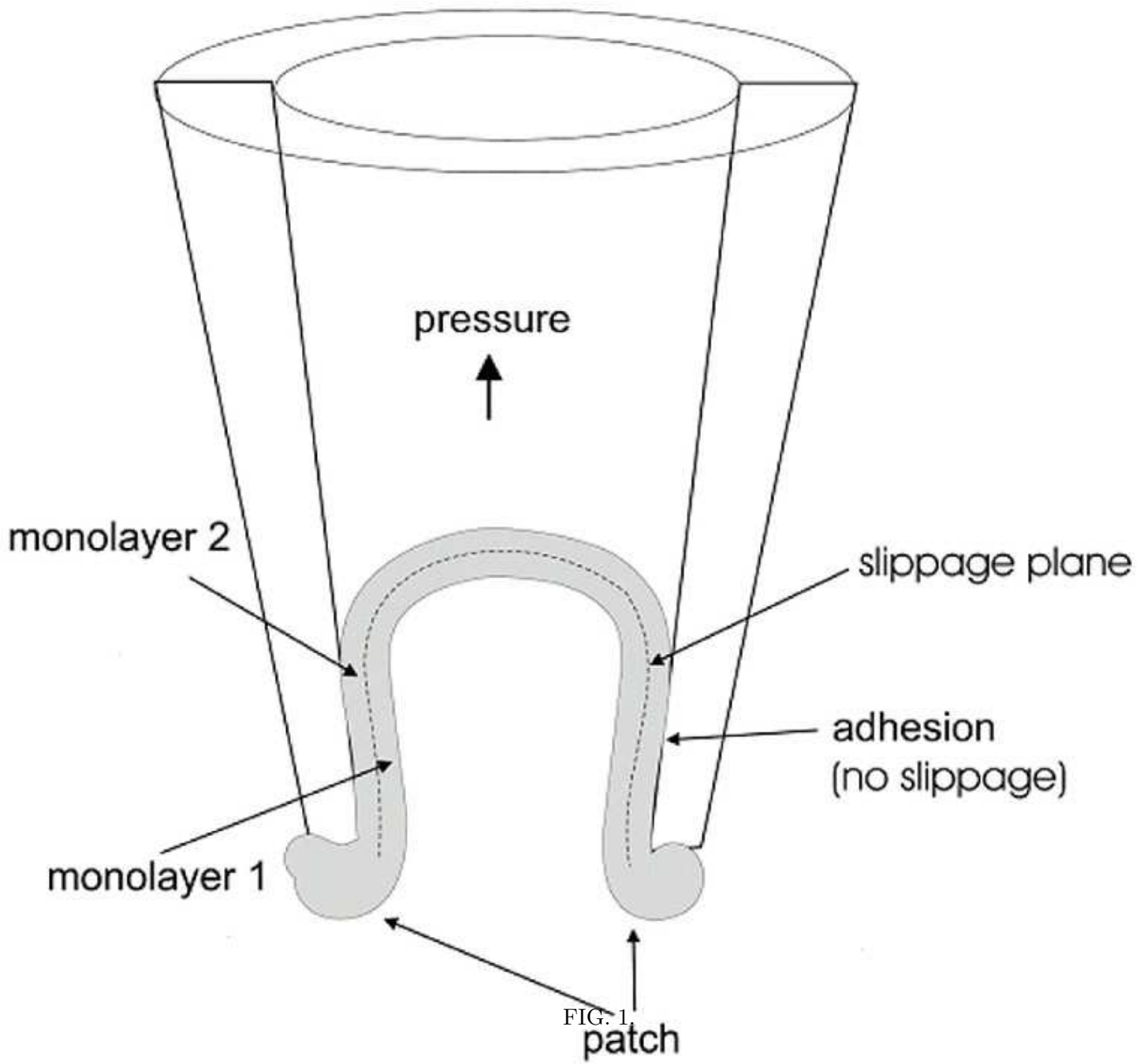
Fig. 3*a*. Normalized areas per lipid molecule at the external surfaces of the monolayers inside the pipette in the semi-equilibrium z_i^{disc}/z_0 and complete equilibrium z_i^{conn}/z_0 state *versus* dimensionless pressure difference p . Other parameters are as in Fig. 2*a*.

Fig. 3*b*. *Dots*: Normalized lateral tension T_1 in the monolayer 1 in the semi-equilibrium state *versus* dimensionless pressure difference p . *Solid line*: Normalized curvature h_{disc}/h_0 of the membrane inside the pipette in the semi-equilibrium state is taken from Fig. 2*c* for a convenience of comparison. Other parameters are as in Fig. 2*a*.

Fig. 4. Sketch of the free energy of MscL as function of the pore area A in the elastic model (Sukharev and Markin, 2001). Solid lines - zero tension $T = 0$. The grey lines indicate free energy at finite tension T . The less intensive are the lines - the greater is the tension.

Fig. 5. The activation energy (barrier) for channel closing, $E_{act,c}$ as a function of the free energy difference between open and closed channel conformations (at zero tension) E_0 . Solid black line corresponds to zero tension $T = 0$; the gray lines correspond to the tensions $T = 6\text{dyn/cm}$ and $T = 12\text{dyn/cm}$ (less intensive line is for the greater tension). The energies are expressed in units of $k_B T_0$. Other parameters: $B_C = 0.22k_B T_0$; $B_O = 2.2k_B T_0$; $A_C = 13\text{nm}^2$; $A_O = 30\text{nm}^2$ (Sukharev, Markin, 2001).

FIGURES



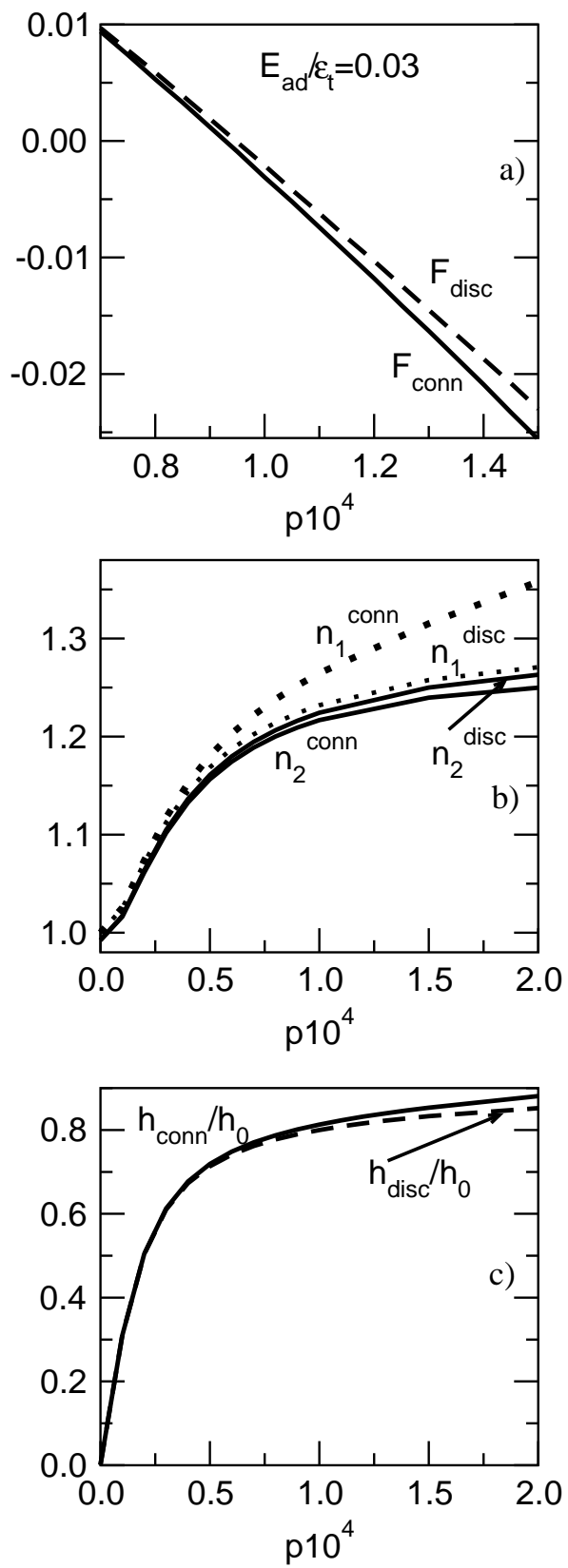


FIG. 2.

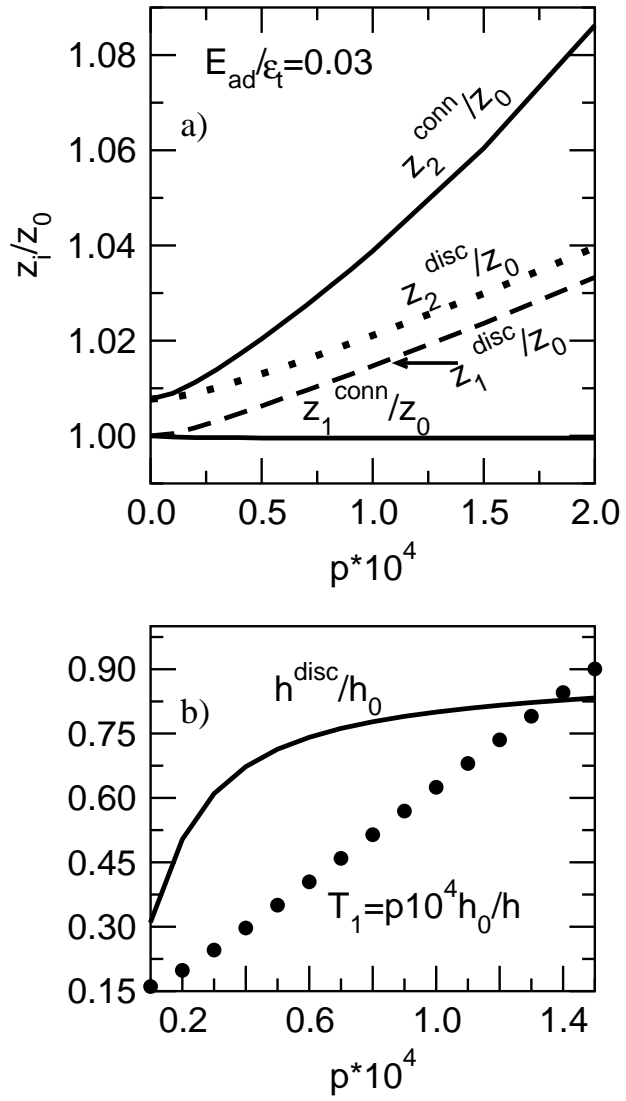


FIG. 3.

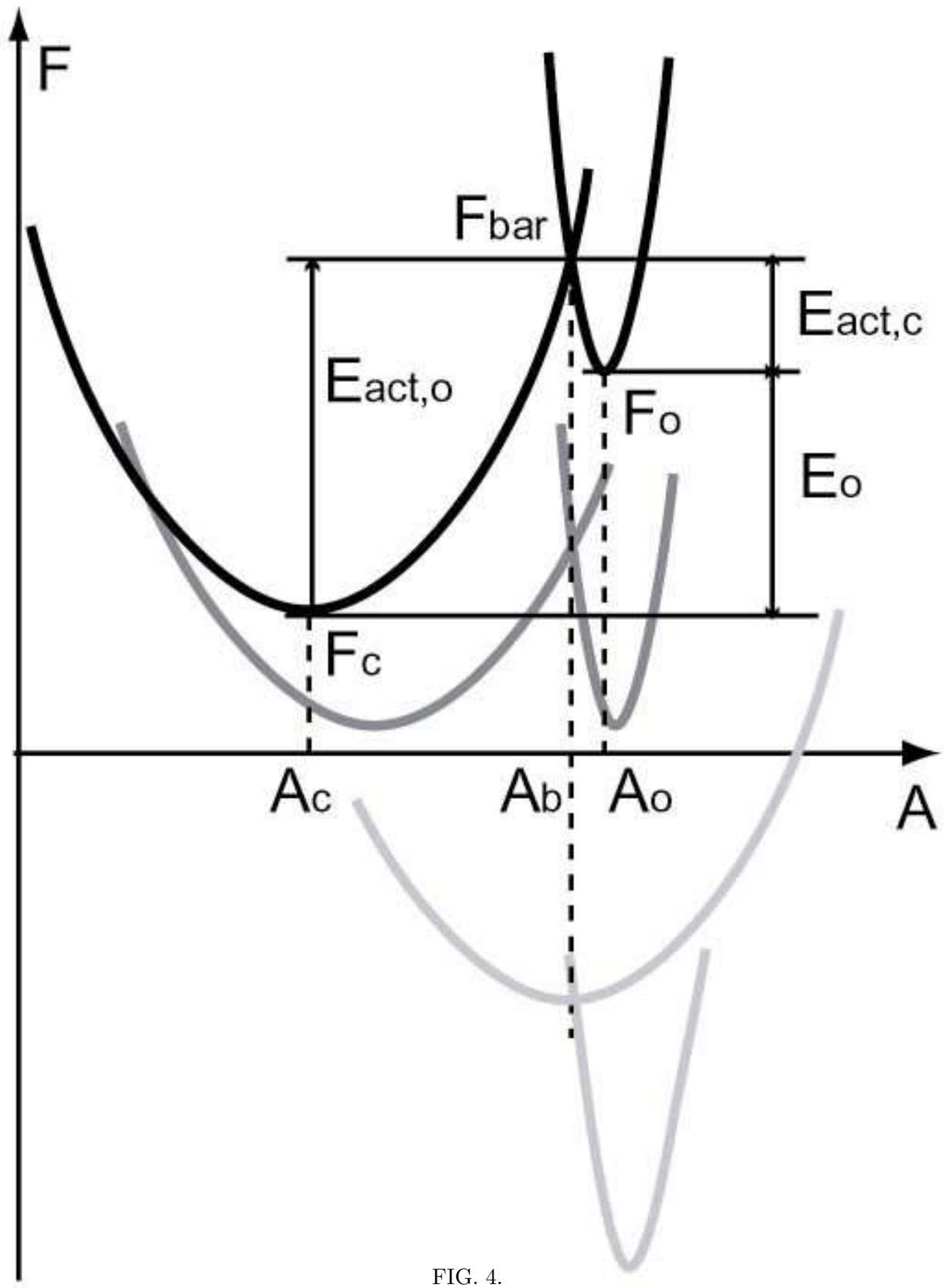


FIG. 4.

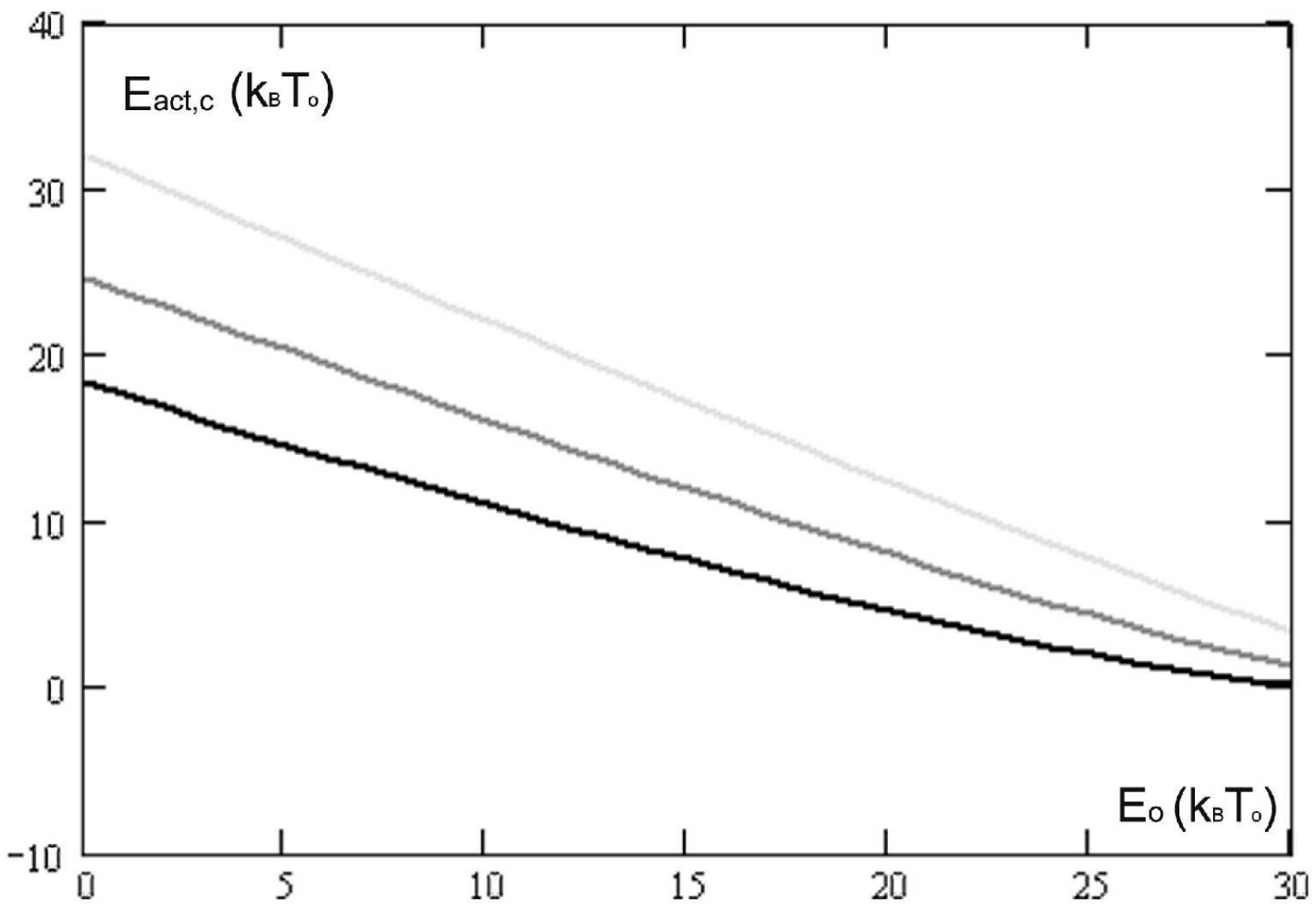


FIG. 5.